© 2015. Published by The Company of Biologists Ltd | Journal of Cell Science (2015) 128, 853–862 doi:10.1242/jcs.118703

RESEARCH ARTICLE

IQGAP1 controls tight junction formation through differential regulation of claudin recruitment

Barbara E. Tanos[1,*,‡,§], Andres E. Perez Bay[1,‡], Susana Salvarezza[1], Igor Vivanco[2,*], Ingo Mellinghoff[2,3,4], Mahasin Osman[5], David B. Sacks[6] and Enrique Rodriguez-Boulan[1,7,§]

ABSTRACT

IQGAP1 is a scaffolding protein previously implicated in adherens junction formation. However, its role in the establishment or maintenance of tight junctions (TJs) has not been explored. We hypothesized that IQGAP1 could regulate TJ formation by modulating the expression and/or localization of junctional proteins, and we systematically tested this hypothesis in the model Madin-Darby canine kidney (MDCK) cell line. We find that IQGAP1 silencing enhances a transient increase in transepithelial electrical resistance (TER) observed during the early stages of TJ formation (Cereijido et al., 1978). Quantitative microscopy and biochemical experiments suggest that this effect of IQGAP1 on TJ assembly is accounted for by reduced expression and TJ recruitment of claudin 2, and increased TJ recruitment of claudin 4. Furthermore, we show that IQGAP1 also regulates TJ formation through its interactor CDC42, because IQGAP1 knockdown increases the activity of the CDC42 effector JNK and dominant-negative CDC42 prevents the increase in TER caused by IQGAP1 silencing. Hence, we provide evidence that IQGAP1 modulates TJ formation by a twofold mechanism: (1) controlling the expression and recruitment of claudin 2 and recruitment of claudin 4 to the TJ, and (2) transient inhibition of the CDC42–JNK pathway.

KEY WORDS: Claudin, IQGAP1, Paracellular permeability, Polarized epithelium, Tight junction

INTRODUCTION

Cell–cell adhesion in polarized epithelia is established and maintained by protein complexes involving tight and adherens junctions, as well as desmosomes (see Nelson, 2003). Tight junction (TJ) formation is crucial for tissue homeostasis, as TJs regulate paracellular permeability in epithelia (gate function) and physically segregate the apical and basolateral domains of epithelial cells (Anderson and Van Itallie, 1995; Cereijido et al., 1998; Mellman and Nelson, 2008; Rodriguez-Boulan and Macara, 2014). The junctional complex has been shown to be compromised in a number of pathological states, including cancer, where impaired cell adhesion seems to be required for tissue invasion and metastasis (Tanos and Rodriguez-Boulan, 2008), as well as bowel inflammatory diseases (Bruewer et al., 2006), diabetic retinopathy (Wallow and Engerman, 1977), macular degeneration (Erickson et al., 2007) and polycystic kidney disease (Yu et al., 2008), where the loss of barrier function disrupts paracellular ion transport homeostasis.

IQGAP1 is a member of a family of scaffolding proteins that interact with signaling and structural molecules (reviewed in Brown and Sacks, 2006) and is highly overexpressed in metastatic breast carcinoma (Jadeski et al., 2008) and glioblastoma (McDonald et al., 2007). It localizes to sites of cell–cell contact in epithelial cells (Fukata et al., 2001) and has been shown to regulate E-cadherin-mediated cell–cell adhesion (Kuroda et al., 1998; Fukata et al., 2001; Li et al., 1999) as well as a number of signal transduction pathways, including Ca^{2+}/calmodulin, (Ho et al., 1999; Ren et al., 2008), CDC42 and Rac (Rittmeyer et al., 2008; Kuroda et al., 1998; Brown and Sacks, 2006; Li et al., 1999) MAPK (Roy et al., 2004; Roy et al., 2005) and mTORC1–Akt (Wang et al., 2009). However, the role of IQGAP1 in TJ assembly and/or maintenance has not been investigated to date.

TJs are composed of scaffolding molecules, such as ZO-1 (also known as TJP1), and transmembrane proteins such as claudins, occludin and junctional adhesion molecules (JAMs) (reviewed in Rahner et al., 2001; Cereijido, 1991; Shin et al., 2006). Barrier function is mainly maintained by claudins, which provide ion selectivity to the gatekeeper properties of the TJ (Van Itallie and Anderson, 2006). Some claudins, such as claudin 2, increase TJ conductivity by forming a Na^{+}-selective pore (Amasheh et al., 2002) (Furuse et al., 2001); others, such as claudin 4, generate pores with broader selectivity and thus cause an overall decrease in ion conductivity (Van Itallie et al., 2001). Ion conductivity can be estimated by measuring transepithelial electrical resistance (TER) (Rahner et al., 2001). TER holds a logarithmic relationship with the number of TJ strands and provides a measurement of TJ establishment and stability (Rahner et al., 2001).

In this study, we find that RNA interference (RNAi)-mediated inactivation of IQGAP1 in Madin-Darby canine kidney (MDCK) cells is sufficient to induce a dramatic increase in TER during TJ formation. Interestingly, analysis of various junctional proteins revealed that IQGAP1 knockdown resulted in enhanced claudin 4 localization and reduced claudin 2 expression and localization to

[1]Department of Ophthalmology, Margaret Dyson Vision Research Institute, Weill Cornell Medical College, New York, NY 10065, USA. [2]Human Oncology & Pathogenesis Program, Memorial Sloan-Kettering Cancer Center, New York, NY 10065, USA. [3]Department of Pharmacology, Weill Cornell Medical College, New York, NY 10065, USA. [4]Department of Neurology, Memorial Sloan-Kettering Cancer Center, New York, NY, USA. [5]Department of Molecular Pharmacology, Physiology and Biotechnology, Division of Biology and Medicine, Alpert School of Medicine, Brown University, Providence, RI 02912, USA. [6]Department of Laboratory Medicine, National Institutes of Health, Bethesda, MD 20892, USA. [7]Department of Cell and Developmental Biology, Weill Cornell Medical College, New York, NY 10065, USA.
*Present address: Division of Cancer Therapeutics, The Institute of Cancer Research, London SM2 5NG, UK.
‡These authors contributed equally to this work

§Authors for correspondence (Barbara.tanos@icr.ac.uk; Boulan@med.cornell.edu)

Received 24 August 2012; Accepted 5 November 2014

Journal of Cell Science (2015) 128, 853–862 doi:10.1242/jcs.118703

TJs, suggesting a mechanism for the observed increase in TER. Furthermore, we find that this increase in TER can be reversed by expression of dominant-negative CDC42, an interactor of IQGAP1. In addition, IQGAP1 knockdown promotes increased activation of JNK, an effector of CDC42. Thus, our study identifies IQGAP1 as an important player in the establishment of TJs and establishes a mechanistic link between IQGAP1, the CDC42–JNK pathway and the spatial regulation of claudins during the early steps in the establishment of epithelial polarity.

RESULTS

IQGAP1 knockdown promotes a transient increase in transepithelial electrical resistance

We first asked whether IQGAP1 protein levels could influence the formation and stability of TJs. To do this, we depleted IQGAP1 from MDCK cells, a model cell line used extensively for the study of epithelial polarity (Cereijido et al., 1978; Rodriguez-Boulan et al., 2005) using RNAi (Rittmeyer et al., 2008). Small interfering (si)RNA oligos were introduced into cells by two consecutive rounds of electroporation and IQGAP1 knockdown was quantified by fluorescent immunoblot, as described in Materials and Methods (Fig. 1A). IQGAP1 has been shown to localize to lateral junctions (Noritake et al., 2004). We confirmed this localization by immunostaining, and found that most of the junction-associated protein was absent from IQGAP1-knockdown cells (Fig. 1B). Next, we analyzed the effects of IQGAP1 knockdown on TJ formation using a Ca^{2+} switch assay (Gonzalez-Mariscal et al., 1990) in which confluent MDCK monolayers are incubated in Ca^{2+}-free medium to completely disrupt cell–cell contacts and then switched to Ca^{2+}-rich medium to allow re-establishment of intercellular contacts. This results in a sequence of Ca^{2+}-dependent E-cadherin–E-cadherin and ZO-1–E-cadherin interactions that concludes with the normal positioning of TJs above the adherens junctions (Rajasekaran et al., 1996). TJ formation can be followed by measuring the transepithelial electrical resistance (TER) over time, which is a measure of their ionic conductance (Cereijido et al., 1978). Early work (Cereijido et al., 1978) has shown that MDCK II cells plated at confluency after dissociation by trypsin develop a TER peak of ~500 ohms.cm^2 before reaching a plateau of ~100–200 ohms.cm^2. We found that 9 h after Ca^{2+} addition, control MDCK monolayers developed a transient TER peak of <500 ohms.cm^2 whereas IQGAP1-knockdown cells showed a much larger TER peak, ranging from 1200 to 2000 ohms.cm^2 (Fig. 1C). This effect was reverted upon transfection of an RNAi-resistant IQGAP1 cDNA (supplementary material Fig. S1). In contrast to the dramatic effect on TER, IQGAP1 knockdown did not affect expression of the TJ marker ZO-1 and the adherens junction protein E-cadherin (supplementary material Fig. S2) or the polarity of several membrane polarity markers (supplementary material Fig. S3).

Transient TER peak requires actin polymerization

The actin cytoskeleton has been shown to be linked to TJ components through the membrane-associated guanylate kinase (MAGUK) family protein ZO-1 (Fanning et al., 1998), and IQGAP1 is known to bind and cross-link actin filaments (Bashour et al., 1997). Thus, we examined whether actin polymerization and turnover could influence the striking effect of IQGAP1 on TJ formation. To this end, we used cytochalasin D, which inhibits actin polymerization by binding to G-actin. We found that inhibition of actin polymerization with cytochalasin D completely suppressed the increase in TER in both control and IQGAP1-knockdown cells (Fig. 2A); therefore, actin polymerization seems to have a broad effect on TJ formation, not just related to IQGAP1. By contrast, the TER increase was not affected by jasplakinolide, a drug that inhibits actin turnover by binding to F-actin (Fig. 2A,C). Importantly, when we analyzed F-actin distribution using phalloidin staining, we found that IQGAP1-knockdown cells did not show any considerable difference in F-actin distribution (Fig. 2C), albeit cells displayed a slightly more columnar morphology (Fig. 2C) and a significant increase in cell height (Fig. 2D), consistent with the idea that IQGAP1 silencing might increase the number of cell–cell junctions in the lateral membrane.

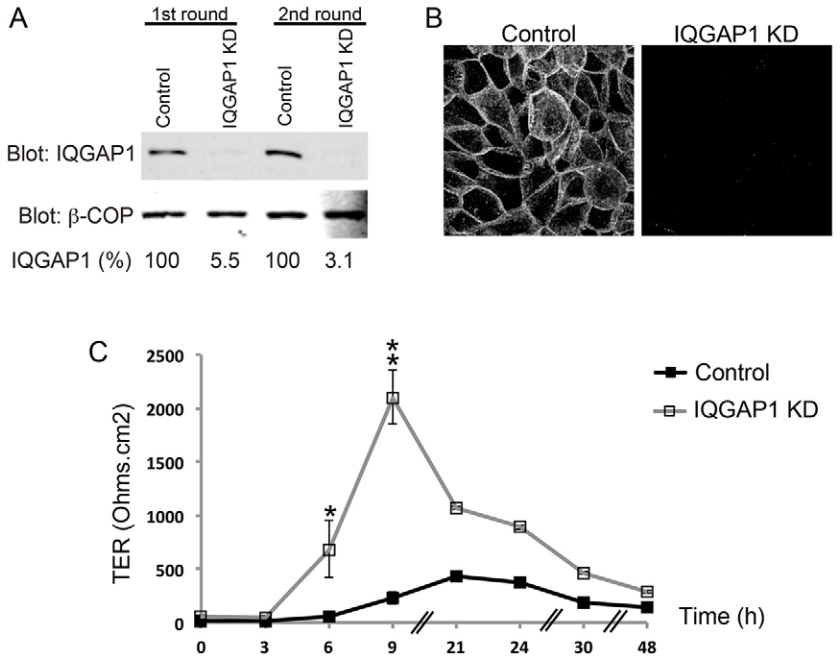

Fig. 1. IQGAP1 knockdown promotes an increase in transepithelial electrical resistance. MDCK II cells were electroporated with control luciferase siRNA or IQGAP1 siRNA. (A) Western blot showing IQGAP1 protein levels in control and IQGAP1-knockdown (KD) cells 3 days after the first round (left) and 3 days after the second round (right) of AMAXA electroporation. IQGAP1 levels normalized to the β-COP loading control are indicated as a percentage (%) relative to control lanes. (B) Maximum projection of a confocal *z*-stack showing control (left) and IQGAP1-knockdown (right) cells immunostained for IQGAP1, 3 days after the second electroporation. Images were acquired using a 63× oil-immersion objective. (C) TER was measured at different times during a Ca^{2+} switch assay in control and IQGAP1-knockdown monolayers. Note the significant differences in TER at 6 and 9 h after the switch to normal Ca^{2+} medium. *P=0.0194; **P=0.0004 (Student's *t*-test of the differences between two means). Data show the mean±s.e.m. (three independent experiments).

Journal of Cell Science (2015) 128, 853–862 doi:10.1242/jcs.118703

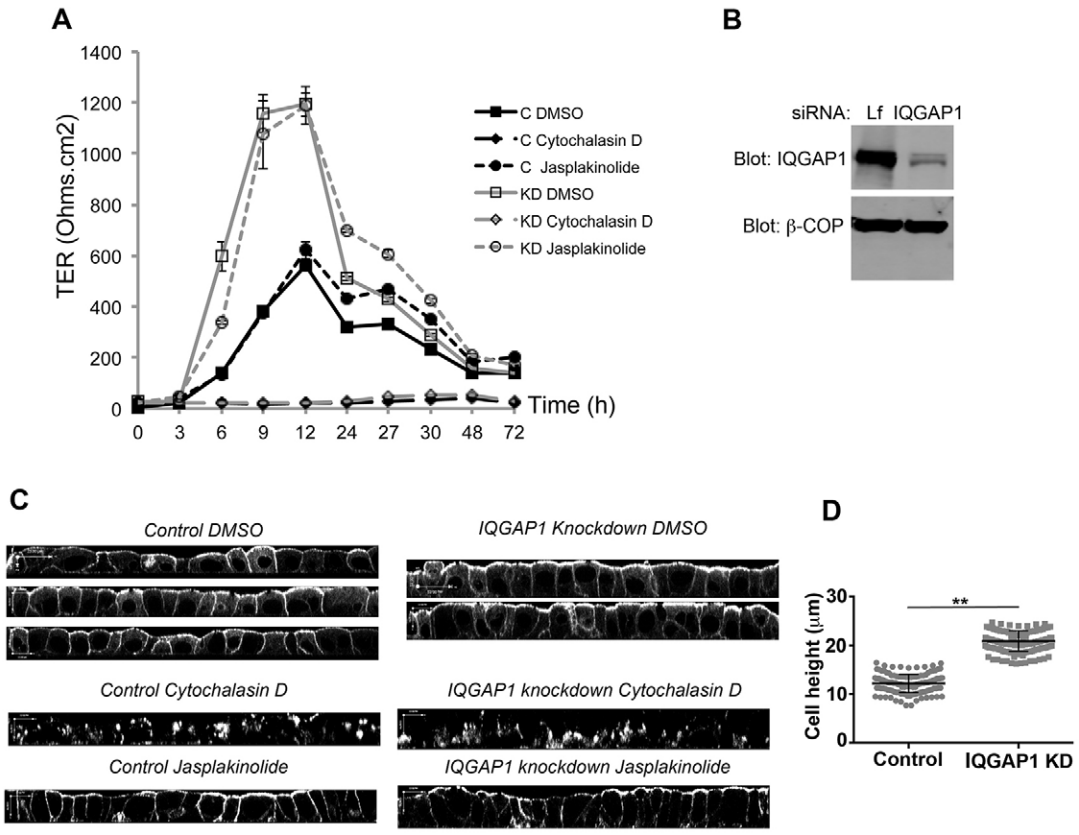

Fig. 2. Transient TER peak requires actin polymerization. (A) TER measurements in control ('C') and IQGAP1-knockdown (KD) monolayers during a Ca^{2+} switch assay, with the addition of DMSO (vehicle control), cytochalasin D (to prevent actin polymerization) and jasplakinolide (to prevent actin turnover). Note that the TER increase requires actin polymerization but not actin turnover. Data show the mean±s.e.m. (three independent experiments). (B) Western blot of lysates from control (Lf) and IQGAP1-knockdown cells from A using anti-IQGAP1 (upper panel) and anti-β-COP (lower panel) antibodies. (C) Confocal images of control and IQGAP1-knockdown MDCK II cells stained with phalloidin to visualize the actin cytoskeleton. Note that IQGAP1-knockdown cells are taller and more columnar than control cells. Images were acquired using a 63× oil-immersion objective. (D) Quantification of the cell height difference observed in C. The horizontal line shows the mean, error bars indicate s.e.m. $^{**}P<0.001$ (Student's *t*-test).

IQGAP1 regulates TJ formation through transient inhibition of the CDC42–JNK pathway

CDC42 has been shown to regulate IQGAP1 activity through direct interaction (Kuroda et al., 1996; Kuroda et al., 1998; Rittmeyer et al., 2008). However, IQGAP1 can also regulate the activation of CDC42 (Rittmeyer et al., 2008). CDC42 is also required for TJ formation (Wallace et al., 2010) and maintenance (Rojas et al., 2001). To investigate the relevance of the IQGAP1–CDC42 interaction in the regulation of TJ formation, we examined their physical association during epithelial cell polarization. Co-immunoprecipitation at different time-points after Ca^{2+} replenishment showed that the interaction between CDC42 and IQGAP1 changed slightly during junction formation, with a decrease at early time-points, including the 9 h time-point, the time at which we observed the TER peak (Fig. 3A). Because CDC42 is thought to promote TJ formation, our data suggest that IQGAP1 could be acting as an inhibitor of CDC42 during this process. Indeed, we found that expression of dominant-negative CDC42 blocked the effects of IQGAP1 knockdown on TER (Fig. 3B), using an MDCK cell line (MDCK-T23) stably expressing a tetracycline-regulated (Tet-Off) dominant-negative allele of *CDC42* (Myc-CDC42-N17) (described in Kazmierczak et al., 2001).

To examine whether other components of the CDC42 pathway could be involved in this TER effect, we focused on Jun-N-terminal-kinase (JNK), a well-documented effector of CDC42 (Teramoto et al., 1996). In airway epithelia, JNK has been shown to be required for the development of TER (Terakado et al., 2011) and for the increase in TER following lung injury (Wray et al., 2009). To test whether JNK activity would be affected by IQGAP1 knockdown, we generated a MDCK cell line with stable IQGAP1 knockdown through retroviral delivery of a short hairpin (sh)RNA and measured JNK activity. Interestingly, IQGAP1-knockdown cells showed increased levels of phosphorylation of c-Jun (the primary substrate of JNK) compared with that of control cells (Fig. 3C). Our findings are consistent with a scenario in which IQGAP1 inhibits TJ formation through inhibition of JNK secondary to inhibition of CDC42. In this scenario, depletion of IQGAP1 derepresses both CDC42 and JNK, thereby increasing TJ strength.

IQGAP1 regulates expression levels and TJ recruitment of claudins 2 and 4 during TJ formation

Our data show that IQGAP1 knockdown increases TER during TJ formation. In the MDCK cell model system, claudin 2 has been shown to increase paracellular permeability and reduce TER (Furuse et al., 2001) (Amasheh et al., 2002), whereas claudin 4 has been shown to have the opposite effect (Van Itallie et al., 2001). Therefore, IQGAP1 might control TER levels by regulating expression and TJ recruitment of these claudins during TJ formation.

Journal of Cell Science (2015) 128, 853–862 doi:10.1242/jcs.118703

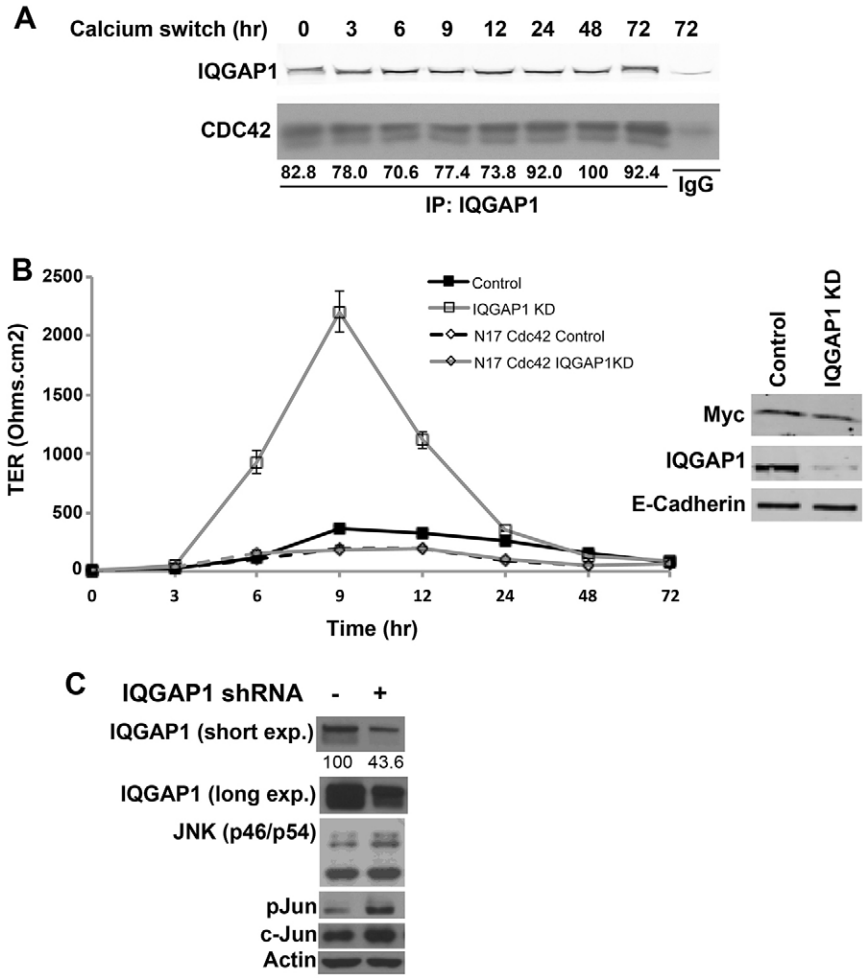

Fig. 3. IQGAP1 interacts with CDC42 during epithelial polarization and controls TJ formation through CDC42. (A) IQGAP1 immunoprecipitation (IP) at different time-points during a synchronized epithelial polarization assay in MDCK cells. Note that CDC42 co-immunoprecipitates with IQGAP1 at all times after the switch to Ca^{2+}-rich medium, but the interaction weakens around the times where we observe higher TER. (B) TER measurements during a Ca^{2+} switch assay in MDCK T23 cells expressing a tetracycline-repressed dominant-negative CDC42 mutant (CDC42 N17). When indicated, doxycycline was removed during the overnight incubation with low-Ca^{2+} medium (16 h) to promote expression of CDC42 N17. The TER peak upon IQGAP1 knockdown (KD) is absent from cells expressing dominant-negative CDC42 N17. Data show the mean±s.e.m. (three independent experiments). The right panel shows a western blot indicating IQGAP1 levels in cells expressing CDC42 N17, electroporated with luciferase siRNA or IQGAP1 siRNA. An E-cadherin loading control is shown in the lower panel. (C) Stable knockdown of IQGAP1 in MDCK cells promotes JNK activation. Lysates from parental MDCK cells and MDCK cells stably transduced with a retroviral IQGAP1-targeted shRNA were analyzed by immunoblot with the indicated antibodies. The percentage expression levels relative to the loading control are indicated.

To study this, we carried out a Ca^{2+} switch assay followed by surface biotinylation at different time-points. Nonpermeable NHS-SS-biotin applied to both apical and basolateral chambers of transwell filters biotinylated lysines of plasma membrane proteins, which were subsequently pulled down with streptavidin beads. Plasma membrane and intracellular proteins contained in pull downs and supernatant, respectively, were separated by SDS-PAGE and blotted for claudins 2 and 4. This assay showed that both intracellular and plasma membrane levels of claudin 2 were almost undetectable at time-point 0, reached half-maximum level between 12 and 25 h and approached plateau by 50 h. Strikingly, these levels were significantly lower in IQGAP1-knockdown cells compared with those of control cells at all time-points studied (Fig. 4A,B; quantification in Fig. 4A′,B′), indicating that IQGAP1 knockdown inhibits both claudin 2 expression and plasma membrane recruitment during TJ formation.

This biochemical approach did not allow us to determine whether IQGAP1 inhibits claudin 2 recruitment specifically to the TJ, because it measures recruitment to the whole plasma membrane. To address this point, we studied the colocalization of claudin 2 and the TJ marker ZO-1 at time-points 0, 9 and 25 h. At time-point 0, claudin 2 fluorescence was not detected, and ZO-1 fluorescence was mostly intracellular, consistent with complete disruption of TJs. By contrast, at time-points 9 and 25 h, claudin 2 and ZO-1 displayed characteristic TJ localization (Fig. 4C–E). Strikingly, the amount of claudin 2 at the TJ was significantly lower in IQGAP1-knockdown compared with control cells, as indicated by the lower Manders colocalization coefficient of ZO-1 pixels occupied by claudin 2 (Fig. 4D′,E′). The percentage of claudin 2 pixels occupied by ZO-1 was not reduced by IQGAP1 knockdown, because IQGAP1 knockdown also reduced the total amount of claudin 2, as determined by assessing claudin 2 mean intensity fluorescence (Fig. 4C′). Taken together, the biochemical and microscopy assays indicate that IQGAP1 knockdown inhibits claudin 2 expression and recruitment to the TJs.

The impaired recruitment of claudin 2 to the TJ might be responsible for the increased TER peak observed in IQGAP1 knockdown. Indeed, claudin-2-knockdown MDCK cells displayed a TER peak similar to that of IQGAP1-knockdown cells and significantly higher than that of control MDCK cells (Fig. 4F), suggesting that IQGAP1 could regulate TER through claudin 2 during TJ formation. Interestingly, double knockdown of IQGAP1 and claudin 2 induced a TER peak even larger than that observed following single knockdown of claudin 2 (Fig. 4F), suggesting that IQGAP1 might only regulate certain aspects of claudin 2 function.

In addition to claudin 2, other claudin family proteins have been shown to regulate paracellular permeability. We focused on claudin 4, which has been shown to reduce paracellular permeability and promote a significant increase in TER (Van Itallie et al., 2001). Biochemical experiments showed that IQGAP1 knockdown did not alter claudin 4 expression during TJ formation (Fig. 5A). This was confirmed by microscopy experiments measuring claudin 4 mean intensity fluorescence

Journal of Cell Science (2015) 128, 853–862 doi:10.1242/jcs.118703

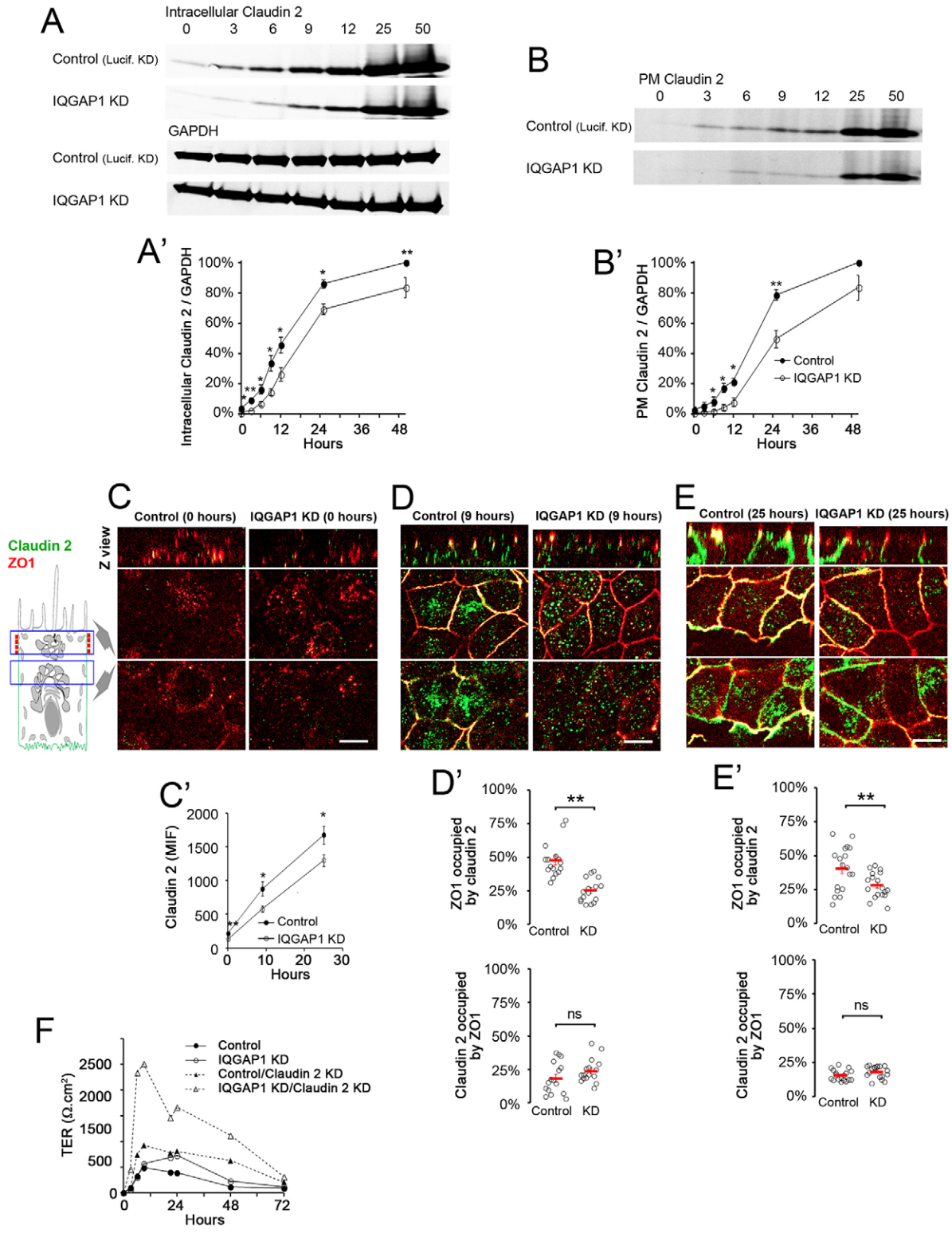

Fig. 4. See next page for legend.

(Fig. 5C′). Plasma membrane recruitment of claudin 4 was increased when measured by cell-surface biotinylation (Fig. 5B); however, low signal prevented us from obtaining accurate quantification. Microscopy experiments confirmed that most of the claudin 4 signal localized intracellularly, with a smaller fraction localizing at the plasma membrane at time-points 9 and 25 h (Fig. 5D,E). Strikingly, the colocalization of claudin 4 and ZO-1 (i.e. ZO-1 pixels occupied by claudin 4 and claudin 4 pixels occupied by ZO-1) was significantly greater in IQGAP1-knockdown cells than control MDCK cells at time-points 9 and 25 h, indicating that IQGAP1 knockdown promotes the recruitment of claudin 4 to the TJ (Fig. 5D′,E′). Taken

Journal of Cell Science (2015) 128, 853–862 doi:10.1242/jcs.118703

Fig. 4. IQGAP1 knockdown reduces expression levels and TJ recruitment of claudin 2 during TJ formation. (A) Western blot indicating intracellular expression levels of claudin 2 (upper panel) and GAPDH (lower panel) in control and IQGAP1-knockdown (KD) MDCK cells at different time-points during a Ca^{2+} switch assay. Lucif., luciferase. (A′) Quantification of the claudin 2:GAPDH ratio from three independent experiments similar to that presented in A. Data show the mean±s.e.m. (B) Western blot indicating expression levels of plasma membrane (PM) claudin 2 in control and IQGAP1-knockdown MDCK cells at different time-points during a Ca^{2+} switch assay. (B′) Quantification of the plasma membrane claudin 2:GAPDH ratio from three independent experiments. Data show the mean±s.e.m. (C–E) Confocal images of control and IQGAP1-knockdown MDCK monolayers at time-points 0, 9 and 25 h, showing claudin 2 colocalization with the TJ marker ZO-1. Note that IQGAP1-knockdown MDCK cells show a substantial decrease in claudin 2 recruitment to the TJ compartment, defined by ZO-1. Scale bars: 10 μm. (C′) Cells from experiments represented in C–E were quantified for claudin 2 mean intensity fluorescence (MIF). (D′,E′) Cells from experiments represented in D,E were quantified for the percentage of pixels of ZO-1 occupied by claudin 2 (upper panel) and the percentage of pixels of claudin 2 occupied by ZO-1 (lower panel). Circles represent values from individual cells and red lines represent the mean value. Error bars indicate ±s.e.m. ns, not significant; $*P<0.05$; $**P<0.001$ (Student's *t*-test). (F) TER measurements during Ca^{2+} switch assays from control, IQGAP1 knockdown, claudin 2 knockdown and double IQGAP1, claudin 2 knockdown MDCK cells.

together, these results indicate that IQGAP1 increases expression levels and TJ recruitment of claudin 2 and inhibits TJ recruitment of claudin 4, which attenuates the TER peak observed during TJ formation.

DISCUSSION

IQGAP1 has been shown to regulate the formation of adherens junctions (Fukata et al., 2001; Li et al., 1999). However, whether IQGAP1 is also implicated in the regulation of TJs has not been addressed. Our data provide the first evidence of an inhibitory role for IQGAP1 in TJ formation during epithelial polarization.

We found that RNAi-mediated downregulation of IQGAP1 led to an increase in TER (Fig. 1). This TER effect was rescued by expression of an RNAi-resistant IQGAP1 cDNA in IQGAP1-knockdown cells (supplementary material Fig. S1). Interestingly, IQGAP1-knockdown cells showed an increased columnar appearance, probably as a result of increased junctional strength (Fig. 2C), and a significant increase in cell height (Fig. 2D). Our analysis showed that these changes were not associated with changes in the levels of a number of junctional proteins such as E-cadherin, occludin and ZO-1 (supplementary material Fig. S2). However, IQGAP1 knockdown had a profound effect on the differential regulation of claudins. Claudin 2 and claudin 4 are two well-studied TJ proteins that have a key role in the regulation of barrier function through their channel activities. Claudin 2 forms a cation-selective pore at the TJ that decreases TER and increases conductivity (Furuse et al., 2001; Amasheh et al., 2002), whereas claudin 4 decreases paracellular conductance by reducing Na^+ permeability (Van Itallie et al., 2001). Notably, we have also found that IQGAP1 knockdown promotes a decrease in the total levels of claudin 2 protein and a decrease in the TJ recruitment of claudin 2 (Fig. 4), which could explain the significant increase in TER in IQGAP1-knockdown cells. Interestingly, our experiments also show that IQGAP1 knockdown promotes an increase in claudin 4 recruitment to TJs (Fig. 5). This differential recruitment of claudins to the TJ could potentially be explained by IQGAP1 effects on membrane trafficking (Osman, 2010).

IQGAP1 has been placed both upstream and downstream of CDC42 and is therefore likely to play an important role in the regulation of this molecule (Kuroda et al., 1996; Kuroda et al., 1998; Kuroda et al., 1999; Rittmeyer et al., 2008). Experiments using mutant alleles of CDC42 revealed that CDC42 regulates early steps of TJ formation (Rojas et al., 2001). Knockdown of CDC42 [or its effectors PAK4 and Par6B (also known as PARD6B)] impairs junction formation in bronchial epithelial cells (Wallace et al., 2010). Our results show that CDC42 interacts with IQGAP1 during TJ formation; however, this interaction seems to be weaker at the time points where we observe a higher TER (Fig. 3A). This is consistent with a scenario in which IQGAP1 inhibits TJ formation by restricting the function of CDC42. Indeed, our results show that the ability of IQGAP1 to regulate barrier function is CDC42 dependent (Fig. 3B); hence, they provide evidence for a link between IQGAP1 function and CDC42-regulated TJ formation.

In airway epithelia, the CDC42 effector JNK has been shown to be required for TJ barrier function (Terakado et al., 2011) and for the increase in TER following lung injury (Wray et al., 2009). Consistently, we found that IQGAP1 knockdown led to activation of JNK in MDCK cells (Fig. 3C), thus supporting a role for JNK in the increase in TJ strength upon IQGAP1 knockdown.

Finally, IQGAP1 is known to interact with Exo70 (also known as EXOC7) (Rittmeyer et al., 2008), a key component of the exocyst complex. As the exocyst is known to regulate basolateral trafficking (Grindstaff et al., 1998), further work could potentially uncover whether IQGAP1 functions at the junctional compartment, modulating protein trafficking to the TJ at specific times during epithelial polarization, maybe through interactions with Exo70 or other trafficking molecules. In support of this view, IQGAP1 has also been shown to interact with septin 2 (Rittmeyer et al., 2008), which functions as a diffusion barrier for protein trafficking to specialized cellular compartments (Hu et al., 2010). However, we did not observe any changes in the localization of several basolateral markers (supplementary material Fig. S3), suggesting that the IQGAP1 effects might be specific for TJ proteins.

In summary, our study supports a model of TJ formation that involves IQGAP1-sensitive differential recruitment of claudin 2 and claudin 4 to the TJ site, and IQGAP1-sensitive activation of CDC42–JNK that likely facilitates junction maturation (Fig. 6). Furthermore, given the prognostic value of claudin 4 total protein expression in various tumor types (Ersoz et al., 2011; Sung et al., 2011; Szasz et al., 2011) and the association between loss of TJs and metastatic behavior (Martin et al., 2011), our results also provide additional evidence that IQGAP1 might be a potential therapeutic target for the treatment of advanced cancers.

MATERIALS AND METHODS

Cell culture

MDCK (strain II) cells were grown in DMEM (Invitrogen) supplemented with 100 U/ml penicillin, 100 mg/ml streptomycin and 5% fetal calf serum (FCS; Invitrogen) at 37℃ in a humidified atmosphere with 5% CO_2. MDCKII T23 cells with inducibly repressed (tet-off) dominant-negative CDC42 were a kind gift from W. James Nelson (Stanford University, CA). For polarization experiments, cells were grown in Transwell chambers with polycarbonate filters (Corning Costar, Tewksbury, MA). 293T cells were grown in DMEM supplemented with 10% FCS and antibiotics.

siRNA-mediated knockdown and permanent silencing of IQGAP1 in MDCK cells

Previously described sequences for siRNA targeting of IQGAP1 (5′-TGCCATGGATGAGATTGGA-3′) (Rittmeyer et al., 2008) and control luciferase siRNA (GL2-siRNA) were synthesized by Dharmacon

Journal of Cell Science (2015) 128, 853–862 doi:10.1242/jcs.118703

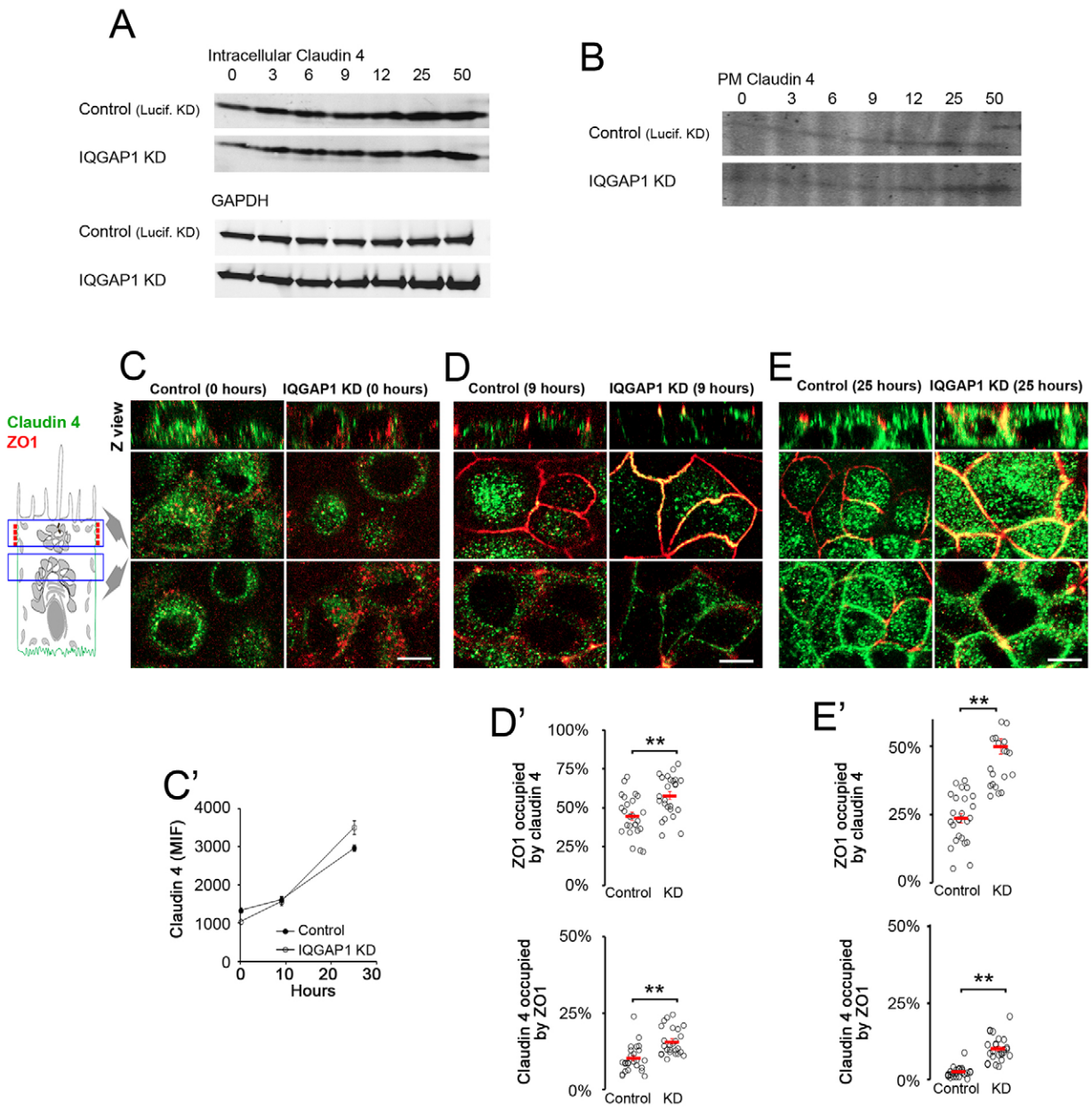

Fig. 5. IQGAP1 knockdown increases TJ recruitment of claudin 4 during TJ formation. (A) Western blot indicating intracellular expression levels of claudin 4 (upper panel) and GAPDH (lower panel) in control and IQGAP1-knockdown (KD) MDCK cells at different time-points during a Ca^{2+} switch assay. Lucif., luciferase. (B) Western blot indicating expression levels of plasma membrane (PM) claudin 4 in control and IQGAP1-knockdown MDCK cells at different time-points during a Ca^{2+} switch assay. (C–E) Confocal images of control and IQGAP1-knockdown MDCK monolayers at time-points 0, 9 and 25 h, showing claudin 4 colocalization with the TJ marker ZO-1. Note that IQGAP1-knockdown MDCK cells show a substantial increase in claudin 4 recruitment to the TJ compartment, defined by ZO-1. Scale bars: 10 µm. (C′) Cells from experiments presented in C–E were quantified for claudin 4 mean intensity fluorescence (MIF). Data show the mean±s.e.m. (D′,E′) Cells from experiments presented in D,E were quantified for the percentage of pixels of ZO-1 occupied by claudin 4 (upper panel) and the percentage of pixels of claudin 4 occupied by ZO-1 (lower panel). Circles represent the values of individual cells and red lines represent the mean value. Error bars show±s.e.m. $^{**}P<0.001$ (Student's *t*-test).

(Lafayette, CO). To transfect siRNAs, MDCK cells were trypsinized and resuspended in Nucleofector solution (Amaxa, Gaithersburg, MD) at 4×10^6 cells per 100 µl. siRNA oligonucleotide (200 pmol) was added to the cell suspension, and samples were electroporated using the T-023 electroporation program. To stably express an IQGAP1 shRNA, MDCK cells were retrovirally transduced with pSuper-IQGAP1 siIQ8 (5′-AGGAGAAAGGCCGAACTAG-3′) (Mataraza et al., 2003) or a Luciferase control plasmid. Briefly, retrovirus was generated by transient co-transfection of 293T cells with a pCL-Ampho packaging plasmid (Imgenex) and pSuper-IQGAP1. MDCK cells were transduced with two rounds of infection with virus-containing supernatants collected at 36 and 60 h after transfection of the virus-producing 293T cells. Stable expressors were derived through antibiotic selection (5 µg/ml puromycin).

Ca^{2+} switch assay

Following two rounds of electroporation, MDCK cells were plated at 0.5×10^6 cells per filter in 1.2-cm Transwell chambers and allowed to attach in Ca^{2+}-containing DMEM (1.8 mM Ca^{2+}) for 24 h. Thereafter, cells were washed three times in Ca^{2+}-free minimum essential medium

Journal of Cell Science (2015) 128, 853–862 doi:10.1242/jcs.118703

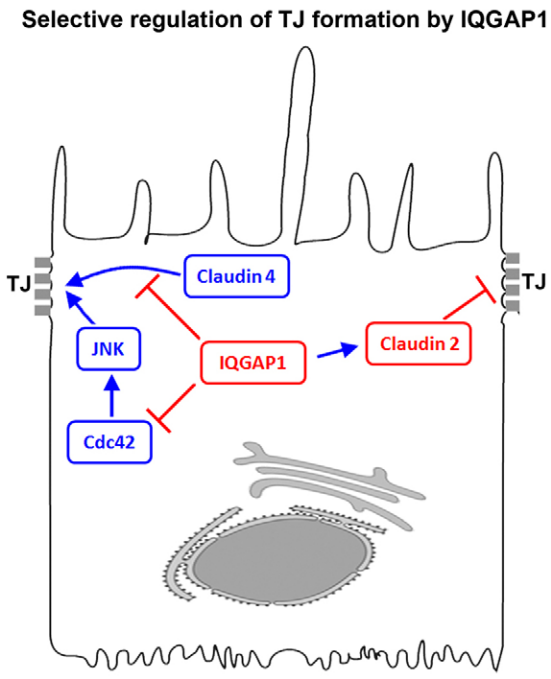

Fig. 6. Model of IQGAP1-regulated TJ formation in polarized epithelia. Positive regulators of barrier function are shown in blue and negative regulators are shown in red. Our results show that the presence of IQGAP1 blocks the early recruitment of claudin 4 to the forming TJs; thus, claudin 4 levels increase upon IQGAP1 knockdown. We propose that IQGAP1 exerts an inhibitory effect on CDC42 during TJ formation, which can also restrict JNK activation, given that JNK is activated following IQGAP1 knockdown. Additionally, IQGAP1 might stabilize claudin 2, which negatively regulates paracellular permeability.

for suspension culture (S-MEM) (Sigma-Aldrich) containing <5 µM Ca^{2+} (low Ca^{2+} medium) and 5% dialyzed fetal bovine serum (FBS) and incubated for ~16 h at 37℃. The medium was then changed back to normal Ca^{2+} medium, to allow the polarization process to begin. This Ca^{2+} switch protocol is essentially as described previously (Gonzalez-Mariscal et al., 1990). The cells were fixed at various time-points in 4% paraformaldehyde (PFA) in PBS for 10 min at room temperature or 4% PFA followed by methanol at −20℃ for 20 min for IQGAP1 immunostaining.

Transepithelial electrical resistance measurements

The TER was measured at the times indicated, on monolayers that were grown on Transwell chambers and subjected to the Ca^{2+} switch protocol, using the EVOM epithelial voltohmeter (World Precision Instruments, Sarasota, FL). Background TER was estimated by measuring the resistance on an empty chamber and was subtracted from each measurement.

Immunofluorescence and confocal microscopy

Briefly, immunofluorescence was performed in cells grown on filters by first fixing cells in 4% PFA at room temperature. Then, after two washes with PBS, the filters were transferred to methanol at −20℃ for 20 min when necessary. Filters were quenched for unreacted aldehydes with 0.1 M glycine, 50 mM ammonium chloride in PBS, permeabilized for 5 min in 1% Triton X-100 in PBS, incubated for 1 h in 10% normal donkey serum (NDS) in PBS and subsequently incubated with primary antibodies in a humid chamber at 4℃ overnight, washed four times with PBS containing 1% Triton X-100 and incubated with secondary antibodies in 5% NDS, washed four times, treated with DAPI for 5 min, washed four times, then mounted on glass slides with Vectashield (Vectorlabs, Burlingame, CA), covered with No. 1.5 coverslips and sealed with nail polish. Laser-scanning confocal microscopy was performed using a Leica TCS SP2 system equipped with argon and helium-neon lasers and, subsequently, a Leica TCS SP5. Images were acquired using a 63× oil-immersion objective, 1.4 numerical aperture, 1024×1024 pixel format, line averaging 4 to reduce noise and sequential scanning. Acquired images were analyzed using Leica software (Leica Microsystems), Metamorph (Molecular Devices), ImageJ and Adobe Photoshop.

Immunoprecipitation, cell-surface biotinylation and western blots

Domain-specific cell-surface biotinylation was performed as described previously (Rodriguez-Boulan et al., 1989) on cells growing in Transwell chambers; after two rounds of biotinylation, cells were lysed in RIPA buffer with protease and phosphatase inhibitors and incubated overnight with streptavidin. For immunoprecipitation experiments, confluent MDCK monolayers grown on Transwell chambers with 2.4-cm or 1.2-cm filter inserts (Corning Costar, Tewksbury MA) and subjected to the Ca^{2+} switch protocol were scraped from the filters with a rubber policeman and lysed in 0.5% NP-40, 0.1 mM EDTA, 20 mM Tris-HCl pH 7.4, 150 mM NaCl, in the presence of phosphatase and protease inhibitors. Lysates were sonicated and centrifuged at 16,100 ***g*** in a microfuge for 20 min. Supernatants (2 mg of protein quantified with Bio-Rad DC reagent, Bio-Rad Laboratories, Hercules, CA), supplemented with 2 µg of anti-IQGAP1 mouse monoclonal antibody and incubated for 2 h, were subsequently incubated with Protein-G–Sepharose beads for an additional 2 h. For cell lysates, 20 µg of protein was separated by SDS-PAGE and transferred to nitrocellulose membrane (Schleicher & Schuell, Keene, NH). Blots were blocked with 5% nonfat dry milk in Tris-buffered saline containing Tween 20 (TBST) and then incubated with primary antibody (diluted in 5% milk/TBST for enhanced chemiluminescence) overnight at 4℃. Western blots were incubated in LICOR blocking reagent for LICOR fluorescent western blots (Li-Cor, Lincoln, Nebraska). After primary antibody incubation, the blots were washed three times with PBS/0.05% Tween 20 and then incubated for 1 h at room temperature with horseradish-peroxidase-conjugated secondary antibody (1:5000 in 5% milk/TBST) or Odyssey blocking buffer (Li-Cor, Lincoln, Nebraska) for Li-Cor western blots. Bound antibody was detected by peroxidase-catalyzed enhanced chemiluminescence (Perkin Elmer Life Sciences, Boston, MA) or with a LICOR Odyssey Infrared Scanner. Densitometric analysis and quantification of the intensity of the individual bands was carried out with Odyssey Software from LICOR.

Mean intensity fluorescence quantification and colocalization analysis

The amount of claudin 2 and claudin 4 was quantified in microscopy experiments as the average mean intensity fluorescence from individual cells in entire confocal stacks, using ZEN 2012 (Zeiss, Thornwood, NY). Three-dimensional colocalization analysis of entire stacks was carried out as described previously (Perez Bay et al., 2013) using the Manders' colocalization coefficient (MCC) (Dunn et al., 2011). MCC provides information on the fraction of marker A occupied by marker B and the fraction of marker B occupied by marker A. To determine the area of marker A (i.e. ZO-1) occupied by marker B (i.e. claudin 2 or 4), we quantified the pixels of marker A colocalizing with marker B and the pixels of marker A in each confocal section of a region of interest (i.e. one cell). These values were summed for all confocal sections of the stack and used to calculate the MCC1 with the formula: pixels of marker A colocalizing with marker B/pixels of marker A. MCC2 was defined by the formula: pixels of marker B colocalizing with marker A/pixels of marker B. Values were expressed as the mean±s.e.m. The statistical method used was the Student's *t*-test. The level of statistical significance is specified for each comparison in the respective figure.

Antibodies and reagents

The sources of the antibodies used in this study were as follows: IQGAP1, E-cadherin and JNK1/2 mouse monoclonal antibodies were purchased from BD Biosciences (San Jose, CA). β-COP antibody was a kind gift from Dr James Rothman (Yale School of Medicine, New Haven,

CT). Actin mouse monoclonal antibody was purchased from Sigma-Aldrich (St Louis, MO). CDC42, c-Jun and Myc antibodies were purchased from Santa Cruz Biotechnology (Santa Cruz, CA). p-Jun (Ser73) antibody was purchased from Millipore (Billerica, MA). Transferrin receptor and Na^+/K^+ ATPase antibodies were purchased from Zymed (San Francisco, CA). Occludin antibody was purchased from Invitrogen (Grand Island, NY) and Exo70 antibody was purchased from Origene (Rockville, MD). GFP antibody was purchased from Clontech (Mountain View, CA). All secondary antibodies were purchased from Jackson Immunoresearch. (West Grove, PA). Cytochalasin D was purchased from Sigma-Aldrich and used at 2 μM. Jasplakinolide (used at 100 nM) was purchased from Calbiochem (San Diego, CA). Phalloidin was purchased from Biotium (Hayward, CA) and used according to the instructions from the manufacturers.

Acknowledgements
We thank Charles Yeaman for reagents and Diego Gravotta, Sylvie Deborde and other members of the Rodriguez-Boulan laboratory for scientific advice.

Competing interests
The authors declare no competing or financial interests.

Author contributions
B.E.T., A.E.P.B., S.S. and I.V. conducted experiments. B.E.T., A.E.P.B., S.S., I.V. and E.R.-B. were responsible for experimental design and data interpretation. M.O., D.B.S and I.M. provided key unpublished reagents and data interpretation. B.E.T. and E.R.-B. wrote the paper.

Funding
This work was supported by grants to E.R.B. from the National Institutes of Health [grant numbers GM-34107 and EY-08538]; by the Dyson Foundation; and by a departmental grant from the Research to Prevent Blindness Foundation. Deposited in PMC for release after 12 months.

Supplementary material
Supplementary material available online at
http://jcs.biologists.org/lookup/suppl/doi:10.1242/jcs.118703/-/DC1

References
Amasheh, S., Meiri, N., Gitter, A. H., Schöneberg, T., Mankertz, J., Schulzke, J. D. and Fromm, M. (2002). Claudin-2 expression induces cation-selective channels in tight junctions of epithelial cells. *J. Cell Sci.* **115**, 4969-4976.

Anderson, J. M. and Van Itallie, C. M. (1995). Tight junctions and the molecular basis for regulation of paracellular permeability. *Am. J. Physiol.* **269**, G467-G475.

Bashour, A. M., Fullerton, A. T., Hart, M. J. and Bloom, G. S. (1997). IQGAP1, a Rac- and Cdc42-binding protein, directly binds and cross-links microfilaments. *J. Cell Biol.* **137**, 1555-1566.

Brown, M. D. and Sacks, D. B. (2006). IQGAP1 in cellular signaling: bridging the GAP. *Trends Cell Biol.* **16**, 242-249.

Bruewer, M., Samarin, S. and Nusrat, A. (2006). Inflammatory bowel disease and the apical junctional complex. *Ann. N. Y. Acad. Sci.* **1072**, 242-252.

Cereijido, M. and Anderson J. (1991). *Tight Junctions*. Boca Raton, FL: CRC Press.

Cereijido, M., Robbins, E. S., Dolan, W. J., Rotunno, C. A. and Sabatini, D. D. (1978). Polarized monolayers formed by epithelial cells on a permeable and translucent support. *J. Cell Biol.* **77**, 853-880.

Cereijido, M., Valdés, J., Shoshani, L. and Contreras, R. G. (1998). Role of tight junctions in establishing and maintaining cell polarity. *Annu. Rev. Physiol.* **60**, 161-177.

Dunn, K. W., Kamocka, M. M. and McDonald, J. H. (2011). A practical guide to evaluating colocalization in biological microscopy. *Am. J. Physiol.* **300**, C723-C742.

Erickson, K. K., Sundstrom, J. M. and Antonetti, D. A. (2007). Vascular permeability in ocular disease and the role of tight junctions. *Angiogenesis* **10**, 103-117.

Ersoz, S., Mungan, S., Cobanoglu, U., Turgutalp, H. and Ozoran, Y. (2011). Prognostic importance of Claudin-1 and Claudin-4 expression in colon carcinomas. *Pathol. Res. Pract.* **207**, 285-289.

Fanning, A. S., Jameson, B. J., Jesaitis, L. A. and Anderson, J. M. (1998). The tight junction protein ZO-1 establishes a link between the transmembrane protein occludin and the actin cytoskeleton. *J. Biol. Chem.* **273**, 29745-29753.

Fukata, M., Nakagawa, M., Itoh, N., Kawajiri, A., Yamaga, M., Kuroda, S. and Kaibuchi, K. (2001). Involvement of IQGAP1, an effector of Rac1 and Cdc42 GTPases, in cell-cell dissociation during cell scattering. *Mol. Cell. Biol.* **21**, 2165-2183.

Furuse, M., Furuse, K., Sasaki, H. and Tsukita, S. (2001). Conversion of zonulae occludentes from tight to leaky strand type by introducing claudin-2 into Madin-Darby canine kidney I cells. *J. Cell Biol.* **153**, 263-272.

Gonzalez-Mariscal, L., Contreras, R. G., Bolívar, J. J., Ponce, A., Chávez De Ramirez, B. and Cereijido, M. (1990). Role of calcium in tight junction formation between epithelial cells. *Am. J. Physiol.* **259**, C978-C986.

Grindstaff, K. K., Yeaman, C., Anandasabapathy, N., Hsu, S. C., Rodriguez-Boulan, E., Scheller, R. H. and Nelson, W. J. (1998). Sec6/8 complex is recruited to cell-cell contacts and specifies transport vesicle delivery to the basal-lateral membrane in epithelial cells. *Cell* **93**, 731-740.

Ho, Y. D., Joyal, J. L., Li, Z. and Sacks, D. B. (1999). IQGAP1 integrates Ca2+/calmodulin and Cdc42 signaling. *J. Biol. Chem.* **274**, 464-470.

Hu, Q., Milenkovic, L., Jin, H., Scott, M. P., Nachury, M. V., Spiliotis, E. T. and Nelson, W. J. (2010). A septin diffusion barrier at the base of the primary cilium maintains ciliary membrane protein distribution. *Science* **329**, 436-439.

Jadeski, L., Mataraza, J. M., Jeong, H. W., Li, Z. and Sacks, D. B. (2008). IQGAP1 stimulates proliferation and enhances tumorigenesis of human breast epithelial cells. *J. Biol. Chem.* **283**, 1008-1017.

Kazmierczak, B. I., Jou, T. S., Mostov, K. and Engel, J. N. (2001). Rho GTPase activity modulates Pseudomonas aeruginosa internalization by epithelial cells. *Cell. Microbiol.* **3**, 85-98.

Kuroda, S., Fukata, M., Kobayashi, K., Nakafuku, M., Nomura, N., Iwamatsu, A. and Kaibuchi, K. (1996). Identification of IQGAP as a putative target for the small GTPases, Cdc42 and Rac1. *J. Biol. Chem.* **271**, 23363-23367.

Kuroda, S., Fukata, M., Nakagawa, M., Fujii, K., Nakamura, T., Ookubo, T., Izawa, I., Nagase, T., Nomura, N., Tani, H. et al. (1998). Role of IQGAP1, a target of the small GTPases Cdc42 and Rac1, in regulation of E-cadherin-mediated cell-cell adhesion. *Science* **281**, 832-835.

Kuroda, S., Fukata, M., Nakagawa, M. and Kaibuchi, K. (1999). Cdc42, Rac1, and their effector IQGAP1 as molecular switches for cadherin-mediated cell-cell adhesion. *Biochem. Biophys. Res. Commun.* **262**, 1-6.

Li, Z., Kim, S. H., Higgins, J. M., Brenner, M. B. and Sacks, D. B. (1999). IQGAP1 and calmodulin modulate E-cadherin function. *J. Biol. Chem.* **274**, 37885-37892.

Martin, T. A., Mason, M. D. and Jiang, W. G. (2011). Tight junctions in cancer metastasis. *Front. Biosci. (Landmark Ed.)* **16**, 898-936.

Mataraza, J. M., Briggs, M. W., Li, Z., Entwistle, A., Ridley, A. J. and Sacks, D. B. (2003). IQGAP1 promotes cell motility and invasion. *J. Biol. Chem.* **278**, 41237-41245.

McDonald, K. L., O'Sullivan, M. G., Parkinson, J. F., Shaw, J. M., Payne, C. A., Brewer, J. M., Young, L., Reader, D. J., Wheeler, H. T., Cook, R. J. et al. (2007). IQGAP1 and IGFBP2: valuable biomarkers for determining prognosis in glioma patients. *J. Neuropathol. Exp. Neurol.* **66**, 405-417.

Mellman, I. and Nelson, W. J. (2008). Coordinated protein sorting, targeting and distribution in polarized cells. *Nat. Rev. Mol. Cell Biol.* **9**, 833-845.

Nelson, W. J. (2003). Epithelial cell polarity from the outside looking in. *News Physiol. Sci.* **18**, 143-146.

Noritake, J., Fukata, M., Sato, K., Nakagawa, M., Watanabe, T., Izumi, N., Wang, S., Fukata, Y. and Kaibuchi, K. (2004). Positive role of IQGAP1, an effector of Rac1, in actin-meshwork formation at sites of cell-cell contact. *Mol. Biol. Cell* **15**, 1065-1076.

Osman, M. (2010). An emerging role for IQGAP1 in regulating protein traffic. *ScientificWorldJournal* **10**, 944-953.

Perez Bay, A. E., Schreiner, R., Mazzoni, F., Carvajal-Gonzalez, J. M., Gravotta, D., Perret, E., Lehmann Mantaras, G., Zhu, Y. S. and Rodriguez-Boulan, E. J. (2013). The kinesin KIF16B mediates apical transcytosis of transferrin receptor in AP-1B-deficient epithelia. *EMBO J.* **32**, 2125-2139.

Rahner, C., Mitic, L. L. and Anderson, J. M. (2001). Heterogeneity in expression and subcellular localization of claudins 2, 3, 4, and 5 in the rat liver, pancreas, and gut. *Gastroenterology* **120**, 411-422.

Rajasekaran, A. K., Hojo, M., Huima, T. and Rodriguez-Boulan, E. (1996). Catenins and zonula occludens-1 form a complex during early stages in the assembly of tight junctions. *J. Cell Biol.* **132**, 451-463.

Ren, J. G., Li, Z. and Sacks, D. B. (2008). IQGAP1 integrates Ca2+/calmodulin and B-Raf signaling. *J. Biol. Chem.* **283**, 22972-22982.

Rittmeyer, E. N., Daniel, S., Hsu, S. C. and Osman, M. A. (2008). A dual role for IQGAP1 in regulating exocytosis. *J. Cell Sci.* **121**, 391-403.

Rodriguez-Boulan, E. and Macara, I. G. (2014). Organization and execution of the epithelial polarity programme. *Nat. Rev. Mol. Cell Biol.* **15**, 225-242.

Rodriguez-Boulan, E., Salas, P. J., Sargiacomo, M., Lisanti, M., Lebivic, A., Sambuy, Y., Vega-Salas, D. and Graeve, L. (1989). Methods to estimate the polarized distribution of surface antigens in cultured epithelial cells. *Methods Cell Biol.* **32**, 37-56.

Rodriguez-Boulan, E., Kreitzer, G. and Müsch, A. (2005). Organization of vesicular trafficking in epithelia. *Nat. Rev. Mol. Cell Biol.* **6**, 233-247.

Rojas, R., Ruiz, W. G., Leung, S. M., Jou, T. S. and Apodaca, G. (2001). Cdc42-dependent modulation of tight junctions and membrane protein traffic in polarized Madin-Darby canine kidney cells. *Mol. Biol. Cell* **12**, 2257-2274.

Roy, M., Li, Z. and Sacks, D. B. (2004). IQGAP1 binds ERK2 and modulates its activity. *J. Biol. Chem.* **279**, 17329-17337.

Roy, M., Li, Z. and Sacks, D. B. (2005). IQGAP1 is a scaffold for mitogen-activated protein kinase signaling. *Mol. Cell. Biol.* **25**, 7940-7952.

Shin, K., Fogg, V. C. and Margolis, B. (2006). Tight junctions and cell polarity. *Annu. Rev. Cell Dev. Biol.* **22**, 207-235.

Sung, C. O., Han, S. Y. and Kim, S. H. (2011). Low expression of claudin-4 is associated with poor prognosis in esophageal squamous cell carcinoma. *Ann. Surg. Oncol.* **18**, 273-281.

Szasz, A. M., Tokes, A. M., Micsinai, M., Krenacs, T., Jakab, C., Lukacs, L., Nemeth, Z., Baranyai, Z., Dede, K., Madaras, L. et al. (2011). Prognostic significance of claudin expression changes in breast cancer with regional lymph node metastasis. *Clin. Exp. Metastasis* **28**, 55-63.

Tanos, B. and Rodriguez-Boulan, E. (2008). The epithelial polarity program: machineries involved and their hijacking by cancer. *Oncogene* **27**, 6939-6957.

Terakado, M., Gon, Y., Sekiyama, A., Takeshita, I., Kozu, Y., Matsumoto, K., Takahashi, N. and Hashimoto, S. (2011). The Rac1/JNK pathway is critical for EGFR-dependent barrier formation in human airway epithelial cells. *Am. J. Physiol.* **300**, L56-L63.

Teramoto, H., Coso, O. A., Miyata, H., Igishi, T., Miki, T. and Gutkind, J. S. (1996). Signaling from the small GTP-binding proteins Rac1 and Cdc42 to the c-Jun N-terminal kinase/stress-activated protein kinase pathway. A role for mixed lineage kinase 3/protein-tyrosine kinase 1, a novel member of the mixed lineage kinase family. *J. Biol. Chem.* **271**, 27225-27228.

Van Itallie, C. M. and Anderson, J. M. (2006). Claudins and epithelial paracellular transport. *Annu. Rev. Physiol.* **68**, 403-429.

Van Itallie, C., Rahner, C. and Anderson, J. M. (2001). Regulated expression of claudin-4 decreases paracellular conductance through a selective decrease in sodium permeability. *J. Clin. Invest.* **107**, 1319-1327.

Wallace, S. W., Durgan, J., Jin, D. and Hall, A. (2010). Cdc42 regulates apical junction formation in human bronchial epithelial cells through PAK4 and Par6B. *Mol. Biol. Cell* **21**, 2996-3006.

Wallow, I. H. and Engerman, R. L. (1977). Permeability and patency of retinal blood vessels in experimental diabetes. *Invest. Ophthalmol. Vis. Sci.* **16**, 447-461.

Wang, J. B., Sonn, R., Tekletsadik, Y. K., Samorodnitsky, D. and Osman, M. A. (2009). IQGAP1 regulates cell proliferation through a novel CDC42-mTOR pathway. *J. Cell Sci.* **122**, 2024-2033.

Wray, C., Mao, Y., Pan, J., Chandrasena, A., Piasta, F. and Frank, J. A. (2009). Claudin-4 augments alveolar epithelial barrier function and is induced in acute lung injury. *Am. J. Physiol.* **297**, L219-L227.

Yu, A. S., Kanzawa, S. A., Usorov, A., Lantinga-van Leeuwen, I. S. and Peters, D. J. (2008). Tight junction composition is altered in the epithelium of polycystic kidneys. *J. Pathol.* **216**, 120-128.

Journal of Cell Science